Chemical Science

ROYAL SOCIETY OF CHEMISTRY

EDGE ARTICLE

View Article Online
View Journal | View Issue

Cite this: *Chem. Sci.*, 2020, **11**, 6889

All publication charges for this article have been paid for by the Royal Society of Chemistry

Crystal engineering of a rectangular sql coordination network to enable xylenes selectivity over ethylbenzene†

Naveen Kumar, ‡[a] Shi-Qiang Wang, ‡[a] Soumya Mukherjee, [a] Andrey A. Bezrukov, [a] Ewa Patyk-Kaźmierczak, [ab] Daniel O'Nolan, [a] Amrit Kumar, [a] Mei-Hui Yu, [c] Ze Chang, [c] Xian-He Bu *[c] and Michael J. Zaworotko *[a]

Separation of the C8 aromatic isomers, *p*-xylene (PX), *m*-xylene (MX), *o*-xylene (OX) and ethylbenzene (EB), is relevant thanks to their widespread application as chemical feedstocks but challenging because of their similar boiling points and close molecular dimensions. Physisorptive separation could offer an energy-efficient solution to this challenge but sorbents which exhibit strong selectivity for one of the isomers remain a largely unmet challenge despite recent reports of OX or PX selective sorbents with high uptake capacity. For example, the square lattice, **sql**, topology coordination network **[Co(bipy)$_2$(NCS)$_2$]$_n$ (sql-1-Co-NCS)** exhibits the rare combination of high OX selectivity and high uptake capacity. Herein we report that a crystal engineering approach enabled isolation of the mixed-linker **sql** coordination network **[Co(bipy)(bptz)(NCS)$_2$]$_n$** (**sql-1,3-Co-NCS**, bipy = 4,4′-bipyridine, bptz = 4,4′-bis(4-pyridyl)tetrazine) and study of its C8 vapour and liquid sorption properties. **sql-1,3-Co-NCS** was found to exhibit high adsorption capacity from liquid xylenes (~37 wt%) and is to our knowledge the first sorbent to exhibit high selectivity for each of xylene isomer over EB ($S_{OX/EB}$, $S_{MX/EB}$, $S_{PX/EB}$ > 5). Insights into the performance of **sql-1,3-Co-NCS** are gained from structural studies which reveal stacking interactions between electron-deficient bptz linkers and the respective xylenes. **sql-1,3-Co-NCS** is the first N-donor mixed-linker **sql** coordination network studied for its gas/vapour sorption properties and represents a large and diverse class of understudied coordination networks.

Received 14th April 2020
Accepted 15th June 2020

DOI: 10.1039/d0sc02123g

rsc.li/chemical-science

Introduction

Separation of C8 aromatics, *p*-xylene (PX), *m*-xylene (MX), *o*-xylene (OX) and ethylbenzene (EB), represents one of the seven industrially critical separation processes "*to change the world*".[1] Whereas C8 aromatic mixtures have utility as anti-knocking additives in gasoline and as solvents for synthetic chemistry, each of the pure isomers are individually relevant:[2] PX is used to manufacture polyethylene terephthalate (PET) and polybutylene terephthalate (PBT); MX is the precursor for isophthalic acid and isophthalic nitrite; OX is converted to phthalic anhydride, an intermediate to coatings and plasticisers; EB is a petrochemical intermediate in production of the resin monomer styrene by dehydrogenation. EB also has utility in the pharmaceutical industry, *e.g.* as a starting material for the drug substances synthomycin and chloramphenicol. The similar molecular sizes and boiling points of C8 aromatics make their separation difficult and energy intensive. Further, formation of eutectics handicaps crystallisation as a purification tool.[2] Distillation is only somewhat feasible for OX removal as it has a relatively high boiling point of 144 °C (PX: 138 °C, MX: 139 °C and EB: 136 °C).[3]

In this context, adsorption based technology involving physisorbents is recognised as offering the potential for reducing the energy footprint of C8 purification.[4,5] However, the state-of-the-art, FAU zeolites, suffer from limited working capacity (~10%) and selectivity (~5).[6] There is a need for new approaches[6,7] as exemplified by Cooper's group, which demonstrated that a flexible pillar[*n*]arene exhibited near-ideal PX selectivity. However, the high selectivity was mitigated by low uptake.[8]

[a]*Department of Chemical Sciences, Bernal Institute, University of Limerick, Limerick V94 T9PX, Republic of Ireland. E-mail: Michael.Zaworotko@ul.ie*

[b]*Faculty of Chemistry, Adam Mickiewicz University, Uniwersytetu Poznanskiego 8, 61-614, Poznan, Poland*

[c]*School of Materials Science and Engineering, Nankai University, Tianjin 300350, P. R. China*

† Electronic supplementary information (ESI) available: Experimental details, crystal structure data, PXRD patterns, TGA curve, *et al.* CCDC 1916015–1916019, 2006768. For ESI and crystallographic data in CIF or other electronic format see DOI: 10.1039/d0sc02123g

‡ These authors contributed equally.

Metal–organic materials (MOMs),[9] also known as metal–organic frameworks (MOFs)[10] or porous coordination polymers (PCPs),[11] have attracted attention thanks to their potential utility in fields such as gas storage/separation, sensing and catalysis.[12–14] That MOMs are modular enables a crystal engineering approach to gain control over the structure of families of related materials to enable systematic structure/property studies.[15,16] In the context of C8 separation, Werner complexes can exhibit OX preference,[17,18] while Bu and co-workers' reported that an L-shaped Ag(I) molecular complex offers benchmark PX selectivity.[19] Unfortunately, these "0D materials" lack the combination of high selectivity (>5) and high working capacity (>50 wt%).[20] Recently, we reported that the previously known coordination network (net) **sql-1-Co-NCS** can behave as a switching adsorbent layered material (SALMA). This square lattice (**sql**) topology net was observed to exhibit benchmark OX capacity (>85 wt%) and OX/EB selectivity (*e.g.* $S_{OX/EB} > 60$).[20] **sql-1-Co-NCS** exhibits switching behaviour as revealed by Type F-IV isotherms[21] that are induced by different C8 isomers at different switching pressures.[20] We attributed the high working capacity of **sql-1-Co-NCS** to its ability to switch between closed and open phases in a manner similar to that of clays. Switching behaviour in **sql** nets was first reported for the related **sql** net $\mathbf{[Cu(bipy)_2(BF_4)_2]_n}$, **ELM-11**, which was observed to exhibit switching in the presence of gases such as CH_4, CO_2, C_2H_2, N_2, O_2 and *n*-butane.[22,23] Surprisingly, **sql** nets remain underexplored with respect to gas/vapour/liquid storage and separation, particularly with respect to C8 aromatics. The linker ligands in **sql** nets typically define pore size/chemistry[24] and linkers such as 4,4′-bis(4-pyridyl)tetrazine (bptz) contain electron-deficient tetrazine rings which are expected to enhance π···π interactions with aromatic hydrocarbons.[25,26] Herein, we report that a crystal engineering strategy[24] involving the use of mixed linker ligands can indeed change pore size/chemistry of **sql** nets and profoundly affect selectivity for C8 aromatics.

sql nets represent 45.09% of reported 2D coordination networks[27] thanks mainly to diverse linker ligand libraries (Fig. S1†). The three most widely used types of linker ligand are as follows: N-donor only (*e.g.* bipy); dicarboxylate (*e.g.* 1,4-benzenedicarboxylate); N-donor-carboxylate bidentate (*e.g.* isonicotinate). They offer three families of single-linker or "Type I" **sql** nets (Fig. 1, left). However, there are also six families of mixed-linker or "Type II" **sql** nets (Fig. 1, right), all of which were introduced[28–33] after the single-linker variants (Fig. S2†).[34–36] Importantly, Type II **sql** nets are amenable to substitution of both linker ligands and their cavities tend to be rectangular rather than square. A survey of the TOPOS TTO∩CSD[37,38] database (see ESI†) revealed that most **sql** nets (>57%) are Type I and that there are relatively few Type II nets with the exception of Type II-ab (1379 entries) (Fig. S3, S4 and Tables S1–S5†). That Type II **sql** nets will offer different pore size and chemistry prompted us to prepare a new Type II-a net, $\mathbf{[Co(bipy)(bptz)(NCS)_2]_n}$ **(sql-1,3-Co-NCS)**. In **sql-1,3-Co-NCS**, half of the bipy linkers are replaced with electron-deficient bptz linkers, allowing us to compare its gas and vapor sorption properties with the parent Type I-a net, $\mathbf{[Co(bipy)_2(NCS)_2]_n}$ **(sql-1-Co-NCS)**. A survey of the literature revealed that only 15 examples of Type II-a **sql** nets have thus far been structurally characterised, none of which were studied for gas/vapour sorption (Table S1†).[28,39–48]

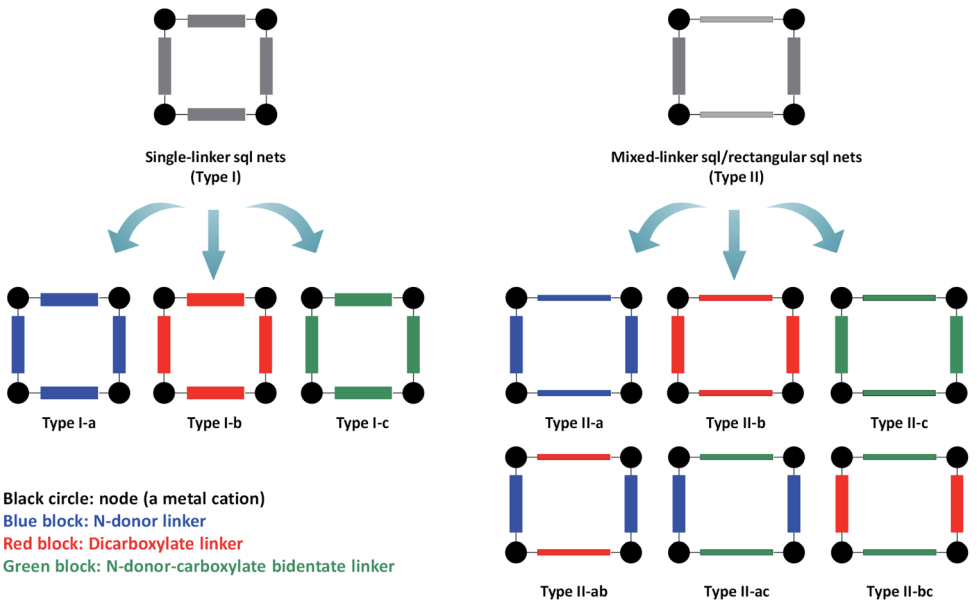

Fig. 1 Classification of **sql** nets based upon single-linker (Type I, left) and mixed-linker (Type II, right) ligands. Type I **sql** nets can be sub-classified according to common linker types as follows: Type I-a = N-donor only; Type I-b = carboxylate donor only; Type I-c = (N-donor-carboxylate bidentate). Type II **sql** nets comprise two different linkers and can be sub-classified as follows: Type II-a = N-donor linker 1 + N-donor linker 2; Type II-b = dicarboxylate linker 1 + dicarboxylate linker 2; Type II-c = (N-donor-carboxylate bidentate) linker 1 + (N-donor-carboxylate bidentate) linker 2; Type II-ab = N-donor linker + dicarboxylate linker; Type II-ac = N-donor linker + (N-donor-carboxylate bidentate) linker; Type II-bc = dicarboxylate linker + (N-donor-carboxylate bidentate) linker.

Experimental section

All reagents were used as received from vendors. Full synthetic procedures and characterisation details are provided in the ESI.†

Synthesis of sql-1,3-Co-NCS·2PX

PX (2 mL) was carefully layered over a solution of bptz (0.015 mmol, 3.5 mg) and bipy (0.015 mmol, 2.3 mg) in 2 mL of dichloromethane. $Co(NCS)_2$ (0.013 mmol, 2.3 mg) in 2 mL of MeOH was then layered on top of PX. Light pink single crystals were obtained after several days with *ca.* 60% yield. The crystals were harvested by filtration and washed with PX three times. **sql-1,3-Co-NCS·2PX** was subsequently prepared in larger scale using a solvothermal method (see ESI† for details).

Synthesis of sql-1,3-Co-NCS·3EtOH

Single crystals of **sql-1,3-Co-NCS·3EtOH** were obtained by soaking crystals of **sql-1,3-Co-NCS·2PX** in 30 mL of EtOH exchanged twice daily over three days.

Synthesis of sql-1,3-Co-NCS

sql-1,3-Co-NCS was prepared by evacuating **sql-1,3-Co-NCS·3EtOH** at 60 °C for 10 hours or degassing **sql-1,3-Co-NCS·3EtOH** using a Micromeritics SmartVacPrep at ambient temperature for 12 hours.

Results and discussion

X-ray crystallography

sql-1,3-Co-NCS·2PX crystallized in the monoclinic space group *C*2/*c* with *ca.* 45% of the lattice volume occupied by PX molecules. The interlayer separation of 5.67 Å is consistent with that of Type I-a bipy-based **sql** nets.[20] Upon exchange with EtOH, **sql-1,3-Co-NCS·2PX** transforms to **sql-1,3-Co-NCS·3EtOH**, which exhibits a reduced interlayer separation of 4.70 Å (Fig. 2) that is just above the interlayer separation of guest-free Type I-a bipy-based **sql** nets.[20] Bulk phase purity of both phases was verified by powder X-ray diffraction (PXRD) (Fig. S5 and S7†). The guest-free or closed phase, **sql-1,3-Co-NCS**, was obtained by activating **sql-1,3-Co-NCS·3EtOH** in vacuum. Unfortunately, attempts to solve the crystal structure of **sql-1,3-Co-NCS** were unsuccessful. The PXRD of activated **sql-1,3-Co-NCS** (Fig. S7†) maintains the major peaks of **sql-1,3-Co-NCS·3EtOH**, however the appearance of new peaks (*e.g.* at 17° and 27°) indicates that a structural

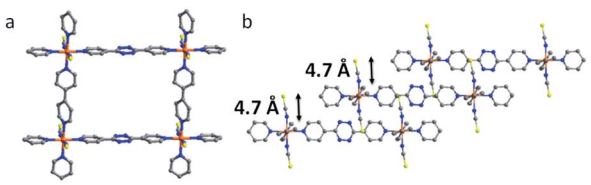

Fig. 2 Crystal structure of **sql-1,3-Co-NCS·3EtOH** with solvent excluded for the sake of clarity: (a) square grid view; (b) layer packing and interlayer separations.

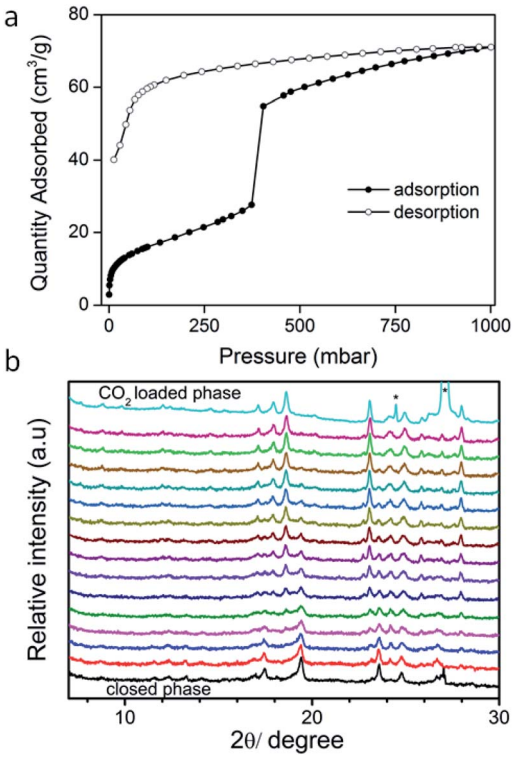

Fig. 3 Activated **sql-1,3-Co-NCS** (closed phase), (a) 195 K CO_2 isotherm; (b) time-dependent (data collection interval: 5 min, 25 min spent on collection of the top CO_2 loaded pattern) *in situ* PXRD patterns recorded upon dosing CO_2 (900 mbar) at 195 K. Peaks labelled * correspond to dry ice.

transformation of **sql-1,3-Co-NCS·3EtOH** resulted from desolvation. The cavity size of **sql-1,3-Co-NCS** is 7.5 × 11.5 Å whereas that of **sql-1-Co-NCS**[20,49] is 7.5 × 7.5 Å. For **sql-1,3-Co-NCS·2PX** and **sql-1,3-Co-NCS·3EtOH**, the square grid angles are ~90°, there is variation in the ∠Co–N–CS angles (Table S10†), the bipy linkers are twisted and the bptz linkers are planar.

CO_2 induced switching behaviour

At 195 K, **sql-1-Co-NCS** was reported to exhibit a switching or Type F-IV[21] CO_2 sorption isotherm at low pressure.[49] **sql-1,3-Co-NCS**, was also observed to exhibit a stepped isotherm (Fig. 3a and S22†) with low CO_2 uptake until *ca.* 350 mbar, at which point gate-opening occurred. Saturation uptake of *ca.* 72 $cm^3\ g^{-1}$ was measured at 1000 mbar. This Type F-II isotherm[21] can be rationalized as a CO_2 induced phase transformation wherein the interlayer separation increases to enable additional CO_2 uptake. To gain insight into the structural changes that accompanied CO_2 sorption and the transformation from closed to open phases, *in situ* PXRD experiments (Fig. 3b) were conducted at 195 K and 900 mbar CO_2. We were unable to index the unit cell of the closed phase but we were able to determine the unit cell parameters for the CO_2 loaded phase **sql-1,3-Co-NCS·*n*CO_2**, which are close to those of **sql-1,3-Co-NCS·3EtOH** (Tables S6 and S8†). The appearance and later disappearance of the additional peak observed at approximately 23° indicates the possible formation of an intermediate phase that accompanies the closed to open phase transition in **sql-1,3-Co-NCS**

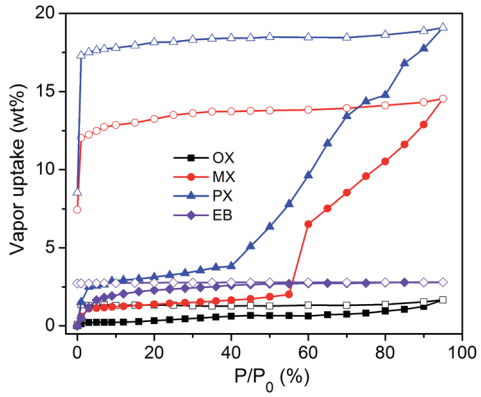

Fig. 4 Xylene vapour sorption isotherms recorded at 298 K for the activated form of **sql-1,3-Co-NCS**.

upon adsorption of CO_2. However, limited powder diffraction data quality (collection time per pattern: 5 min) precludes a detailed structural analysis (Fig. 3b).

Vapour sorption of C8 aromatics

Dynamic vapour sorption studies resulted in Type F-II[21] isotherms for PX and MX, but negligible uptakes for OX and EB (Fig. 4). PX and MX did not reach saturation. The PX and MX uptakes of **sql-1,3-Co-NCS** were measured to be *ca.* 19 and 13 wt%, respectively. These values are consistent with one PX or MX molecule adsorbed per formula unit till *ca.* 95% relative vapour pressure. Soaking experiments (Fig. S11†) revealed very different uptake values. Thermogravimetric analysis (TGA) (Fig. S19†) suggested that **sql-1,3-Co-NCS** adsorbed two PX, MX and OX molecules per formula unit (37 wt%) but only one molecule of EB (18.7 wt%).

Separation of C8 aromatics

That different switching pressures and/or adsorption rates were observed in **sql-1,3-Co-NCS** *vs.* **sql-1-Co-NCS**[20] suggested to us that **sql-1,3-Co-NCS** might be suitable for physisorptive separation of C8 aromatics. Vapour-phase binary mixture separation experiments were conducted on **sql-1,3-Co-NCS** at 85 °C and selectivities were determined by ^{1}H NMR (Fig. S31–S36†) to be very low (1.1 for MX/OX, MX/PX, PX/OX, MX/EB, 1.2 for OX/EB and 1.3 for PX/EB). Liquid phase binary mixtures afforded very different selectivity values (Fig. S37–S42†). Although there no preference for OX/MX, OX/PX or MX/PX was observed, PX/EB, MX/EB and OX/EB selectivities were 9.8, 10.8 and 7.9 respectively (Table S9†). Whereas **sql-1,3-Co-NCS** is less selective for OX/EB than **sql-1-Co-NCS**, its values are comparable to the OX/EB selectivities of **MIL-47(V)**[50] and **MIL-53(Al)**.[51] (Fig. 5). In terms of MX/EB selectivity, **sql-1,3-Co-NCS** is more selective than **sql-1-Co-NCS** (Fig. 5 and Table S9†) and 1.5 times higher than current benchmarks NaY microcrystalline and NaY nanocrystalline (Fig. 5 and Table S9†).[20,52] PX/EB selectivity is also higher than **sql-1-Co-NCS** and equal to the current benchmark **MIL-47(V)**.[20,50] Thus, **sql-1,3-Co-NCS** is the first xylene sorbent to exhibit selectivity >5 over EB for all three xylene isomers.

Structural insights into high xylenes selectivity and uptake

To understand the driving force for the observed xylene selectivity and high working capacities, we determined the crystal structures of the PX and MX loaded phases of **sql-1,3-Co-NCS**. As illustrated in Fig. 6a and b, two PX or MX molecules reside in the interlayer spaces which account for >40% of the unit cell volumes of the corresponding apohost lattices. The calculated PX and MX uptakes from their single crystal structures, 37%, are consistent with the soaking experiments (Fig. 6e). PX and MX molecules exhibit C–H···π and π···π stacking interactions (Fig. 6a and b) with the electron-deficient tetrazine moiety facilitating π···π stacking with the xylene rings. Interestingly, **MIL-47(V)**[50] exhibits similar packing of xylene molecules. That EB does not form π···π stacking interactions with **MIL-47(V)**[50] was possibly a key driving force behind its OX/EB and PX/EB selectivities but the MX/EB selectivity of **MIL-47(V)** is <5. We attribute the improved performance of **sql-1,3-Co-NCS** *vs.* **MIL-47(V)** to enhanced π···π stacking enabled by the tetrazine moieties. This assertion is supported by the experimental studies of Oxtoby *et al.* and the theoretical studies by Wang *et al.* which revealed that tetrazine moieties are electron-deficient with respect to phenyl rings and hence can exhibit stronger π···π stacking interactions with aromatic hydrocarbons.[25,26]

Multiple attempts to obtain single crystals of **sql-1,3-Co-NCS** loaded with OX and EB were unsuccessful. Rather, a stoichiometric

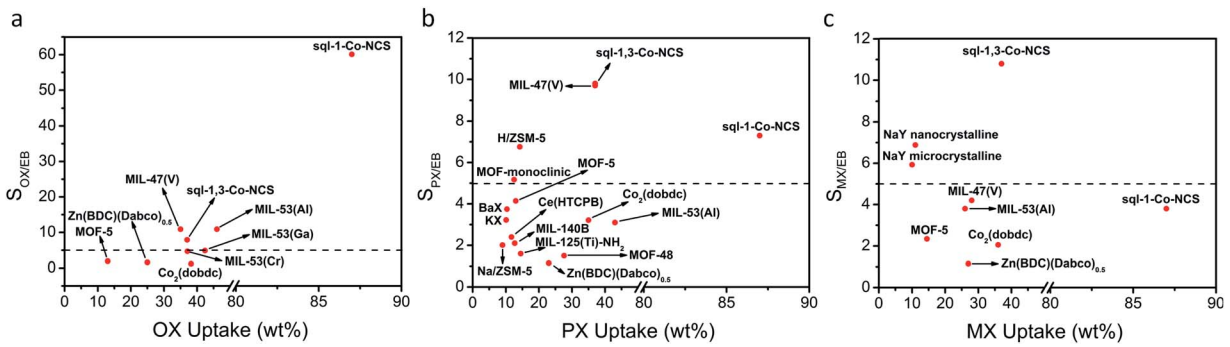

Fig. 5 Comparison of MOMs and zeolites with respect to their (a) OX, (b) PX and (c) MX adsorption capacities and selectivities towards pure xylene isomers *vs.* EB, respectively.

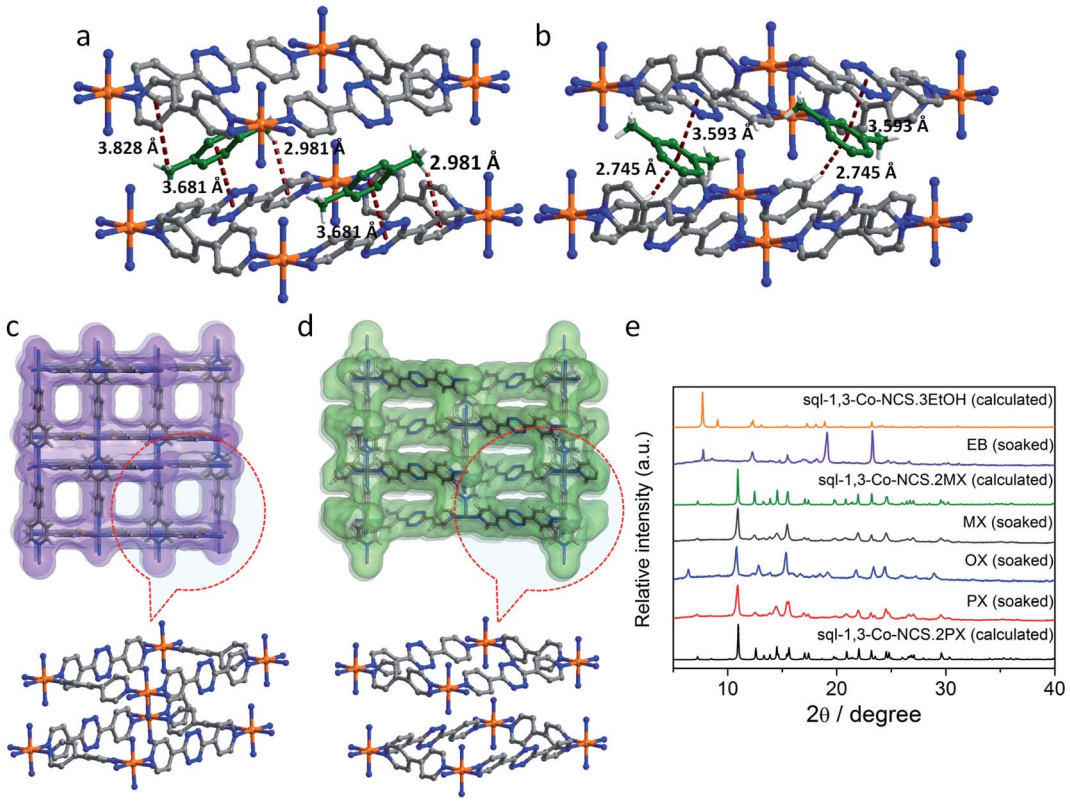

Fig. 6 (a and b) Host–guest interactions in the PX and MX loaded phases, respectively; (c and d) the Connolly surfaces of **sql-1,3-Co-NCS**·3EtOH and **sql-1,3-Co-NCS**·2PX respectively, with a probe radius of 1.4 Å. (e) PXRD patterns for the solvent soaking experiments in pure xylenes and ethylbenzene.

mixture of **sql-1-Co-NCS** and **sql-3-Co-NCS** nets was observed (Fig. S9 and S10†). We were, however, able to determine the unit cell parameters of the OX loaded phase (Table S8†) from Pawley profile fit of the PXRD patterns (Fig. S16†). Unit cell parameters match those of the PX and MX loaded phases (Table S6†) whereas unit cell volumes of 3986(6) $Å^3$, 4007.3(3) $Å^3$ and 4031.0(6) $Å^3$ were determined for the OX, PX and MX loaded phases, respectively. Minor differences between the PXRD pattern of the OX loaded *vs.* the PX/MX loaded phases (Fig. 6e) can be explained by lower symmetry of the OX loaded phase (space group *P*2 *vs.* *C*2/*c* for the PX/MX loaded phases). In particular, the 001 reflection at ~6.4° is not observed in PXRD patterns of the PX/MX loaded variants as this reflection is systematically absent in the latter phases. The PXRD patterns of the EB loaded phase differs from the xylene loaded phases (Fig. 6e). Rather, it matches **sql-1,3-Co-NCS**·3EtOH. The presence of three EtOH molecules per formula unit in the host framework is supported by TGA data (Fig. S17†). As discussed above, **sql-1,3-Co-NCS**·3EtOH exhibits a lower interlayer separation and lower void volume by *ca.* 30%. That the PXRD pattern of the EB loaded phase is similar to the EtOH loaded phase allowed us to deduce how EB interacts with the host framework given that TGA indicates one EB molecule in **sql-1,3-Co-NCS** (Fig. S19 and S21†). The Connolly surfaces of **sql-1,3-Co-NCS**·3EtOH (Fig. 6c) and **sql-1,3-Co-NCS**·2PX (Fig. 6d) reveal that the tetrazine moieties have very different orientations. With respect to the former, pores are not continuous and the tetrazine moieties are not oriented to enable π···π stacking. For the latter, pores are continuous and the tetrazine moieties enable π···π stacking with aromatic guests.

Conclusions

In summary, we report that a mixed-linker crystal engineering approach afforded the new rectangular **sql** coordination net, **sql-1,3-Co-NCS**, and enabled study of its sorption properties, the first sorption studies conducted upon an N-donor mixed-linker **sql** net. **sql-1,3-Co-NCS** was found to exhibit high adsorption capacity for xylenes (~37 wt%) and it is the first sorbent of any type to exhibit high selectivity for all three xylenes over EB (>5). Crystallographic analysis of the guest loaded phases of **sql-1,3-Co-NCS** revealed that the electron-deficient tetrazine moieties play a key role in defining host–guest interactions. It is notable that the observed selectivities are very different from those of its parent, **sql-1-Co-NCS**. The high degree of modularity in mixed-linker **sql** nets is therefore not just of interest from a crystal engineering viewpoint, but also from the perspectives of molecular recognition and selective physisorption.

Conflicts of interest

The authors have no conflicts of interest to declare.

Acknowledgements

M. J. Z. acknowledges the support of the Science Foundation Ireland (SFI Awards 13/RP/B2549 and 16/IA/4624) and the Irish Research Council (IRCLA/2019/167). Z. C. and X.-H. B. acknowledge the National Science Foundation of China (NSFC) (21531005), and the Programme of Introducing Talents of Discipline to Universities (B18030).

References

1 R. P. Lively and D. S. Sholl, *Nature*, 2016, **532**, 435–437.
2 M. A. Moreira, A. F. P. Ferreira, J. C. Santos, J. M. Loureiro and A. E. Rodrigues, *Chem. Eng. Technol.*, 2014, **37**, 1483–1492.
3 C. E. Webster, R. S. Drago and M. C. Zerner, *J. Am. Chem. Soc.*, 1998, **120**, 5509–5516.
4 E. S. Sanz-Pérez, C. R. Murdock, S. A. Didas and C. W. Jones, *Chem. Rev.*, 2016, **116**, 11840–11876.
5 M. Oschatz and M. Antonietti, *Energy Environ. Sci.*, 2018, **11**, 57–70.
6 Y. Yang, P. Bai and X. Guo, *Ind. Eng. Chem. Res.*, 2017, **56**, 14725–14753.
7 X. Zhao, Y. Wang, D.-S. Li, X. Bu and P. Feng, *Adv. Mater.*, 2018, **30**, 1705189.
8 K. Jie, M. Liu, Y. Zhou, M. A. Little, A. Pulido, S. Y. Chong, A. Stephenson, A. R. Hughes, F. Sakakibara, T. Ogoshi, F. Blanc, G. M. Day, F. Huang and A. I. Cooper, *J. Am. Chem. Soc.*, 2018, **140**, 6921–6930.
9 J. J. Perry IV, J. A. Perman and M. J. Zaworotko, *Chem. Soc. Rev.*, 2009, **38**, 1400–1417.
10 S. R. Batten, S. M. Neville and D. R. Turner, in *Coordination Polymers: Design, Analysis and Application*, The Royal Society of Chemistry, 2009.
11 S. Kitagawa, R. Kitaura and S.-I. Noro, *Angew. Chem., Int. Ed.*, 2004, **43**, 2334–2375.
12 J.-R. Li, R. J. Kuppler and H.-C. Zhou, *Chem. Soc. Rev.*, 2009, **38**, 1477–1504.
13 J. Lee, O. K. Farha, J. Roberts, K. A. Scheidt, S. T. Nguyen and J. T. Hupp, *Chem. Soc. Rev.*, 2009, **38**, 1450–1459.
14 Z. Bao, G. Chang, H. Xing, R. Krishna, Q. Ren and B. Chen, *Energy Environ. Sci.*, 2016, **9**, 3612–3641.
15 B. Moulton and M. J. Zaworotko, *Chem. Rev.*, 2001, **101**, 1629–1658.
16 T. R. Cook, Y.-R. Zheng and P. J. Stang, *Chem. Rev.*, 2013, **113**, 734–777.
17 M. Lusi and L. J. Barbour, *Angew. Chem., Int. Ed.*, 2012, **51**, 3928–3931.
18 A. M. Kaluza, S. Mukherjee, S.-Q. Wang, D. J. O'Hearn and M. J. Zaworotko, *Chem. Commun.*, 2020, **56**, 1940–1943.
19 N. Sun, S.-Q. Wang, R. Zou, W.-G. Cui, A. Zhang, T. Zhang, Q. Li, Z.-Z. Zhuang, Y.-H. Zhang, J. Xu, M. J. Zaworotko and X.-H. Bu, *Chem. Sci.*, 2019, **10**, 8850–8854.
20 S.-Q. Wang, S. Mukherjee, E. Patyk-Kaźmierczak, S. Darwish, A. Bajpai, Q.-Y. Yang and M. Zaworotko, *Angew. Chem., Int. Ed.*, 2019, **58**, 6630–6634.
21 Q.-Y. Yang, P. Lama, S. Sen, M. Lusi, K.-J. Chen, W.-Y. Gao, M. Shivanna, T. Pham, N. Hosono, S. Kusaka, J. J. Perry IV, S. Ma, B. Space, L. J. Barbour, S. Kitagawa and M. J. Zaworotko, *Angew. Chem., Int. Ed.*, 2018, **57**, 5684–5689.
22 T. Suzuki, R. Kotani, A. Kondo and K. Maeda, *J. Phys. Chem. C*, 2016, **120**, 21571–21579.
23 A. Kondo, H. Noguchi, S. Ohnishi, H. Kajiro, A. Tohdoh, Y. Hattori, W.-C. Xu, H. Tanaka, H. Kanoh and K. Kaneko, *Nano Lett.*, 2006, **6**, 2581–2584.
24 R. Haldar and T. K. Maji, *CrystEngComm*, 2013, **15**, 9276–9295.
25 N. S. Oxtoby, A. J. Blake, N. R. Champness and C. Wilson, *CrystEngComm*, 2003, **5**, 82–86.
26 W. Wang and P. Hobja, *ChemPhysChem*, 2008, **9**, 1003–1009.
27 T. G. Mitina and V. A. Blatov, *Cryst. Growth Des.*, 2013, **13**, 1655–1664.
28 M.-L. Tong, X.-M. Chen, X.-L. Yu and T. C. W. Mak, *J. Chem. Soc., Dalton Trans.*, 1998, 5–6.
29 L. R. MacGillivray, R. H. Groeneman and J. L. Atwood, *J. Am. Chem. Soc.*, 1998, **120**, 2676–2677.
30 R. H. Groeneman, L. R. MacGillivray and J. L. Atwood, *Chem. Commun.*, 1998, 2735–2736.
31 Y.-T. Wang, H.-H. Fan, H.-Z. Wang and X.-M. Chen, *Inorg. Chem.*, 2005, **44**, 4148–4150.
32 Z.-P. Deng, W. Kang, L.-H. Huo, H. Zhao and S. Gao, *Dalton Trans.*, 2010, **39**, 6276–6284.
33 P. Thuéry, *Inorg. Chem.*, 2011, **50**, 1898–1904.
34 H. Steinfink and G. D. Brunton, *Inorg. Chem.*, 1970, **9**, 2112–2115.
35 P. W. Carreck, M. Goldstein, E. M. McPartlin and W. D. Unsworth, *J. Chem. Soc. D*, 1971, 1634–1635.
36 D. Chackraburtty, *Acta Crystallogr.*, 1957, **10**, 128.
37 V. A. Blatov, A. P. Shevchenko and D. M. Proserpio, *Cryst. Growth Des.*, 2014, **14**, 3576–3586.
38 C. R. Groom, I. J. Bruno, M. P. Lightfoot and S. C. Ward, *Acta Crystallogr., Sect. B: Struct. Sci., Cryst. Eng. Mater.*, 2016, **72**, 171–179.
39 K. Biradha and M. Fujita, *Chem. Commun.*, 2001, 15–16.
40 E. Barea, M. Quirós, J. A. R. Navarro and J. M. Salas, *Dalton Trans.*, 2005, 1743–1746.
41 D. M. Shin, I. S. Lee and Y. K. Chung, *Cryst. Growth Des.*, 2006, **6**, 1059–1061.
42 M. Quesada, F. Prins, O. Roubeau, P. Gamez, S. J. Teat, P. J. van Koningsbruggen, J. G. Haasnoot and J. Reedijk, *Inorg. Chim. Acta*, 2007, **360**, 3787–3796.
43 Y.-W. Li, W.-L. Chen, Y.-H. Wang, Y.-G. Li and E.-B. Wang, *J. Solid State Chem.*, 2009, **182**, 736–743.
44 S.-T. Zheng, Y. Li, T. Wu, R. A. Nieto, P. Feng and X. Bu, *Chem.–Eur. J.*, 2010, **16**, 13035–13040.
45 Y.-M. Jung, *Bull. Korean Chem. Soc.*, 2010, **31**, 2668–2671.
46 M. Khanpour, A. Morsali and P. Retailleau, *Polyhedron*, 2010, **29**, 1520–1524.
47 F. Li, J. K. Clegg and C. J. Kepert, *J. Inclusion Phenom. Macrocyclic Chem.*, 2011, **71**, 381–388.
48 Y.-C. Chuang, C.-T. Liu, C.-F. Sheu, W.-L. Ho, G.-H. Lee, C.-C. Wang and Y. Wang, *Inorg. Chem.*, 2012, **51**, 4663–4671.
49 S.-Q. Wang, Q.-Y. Yang, S. Mukherjee, D. O'Nolan, E. Patyk-Kaźmierczak, K.-J. Chen, M. Shivanna, C. Murray, C. C. Tang and M. J. Zaworotko, *Chem. Commun.*, 2018, **54**, 7042–7045.

50 L. Alaerts, C. E. A. Kirschhock, M. Maes, M. A. van der Veen, V. Finsy, A. Depla, J. A. Martens, G. V. Baron, P. A. Jacobs, J. F. M. Denayer and D. E. De Vos, *Angew. Chem., Int. Ed.*, 2007, **46**, 4293–4297.

51 L. Alaerts, M. Maes, L. Giebeler, P. A. Jacobs, J. A. Martens, J. F. M. Denayer, C. E. A. Kirschhock and D. E. De Vos, *J. Am. Chem. Soc.*, 2008, **130**, 14170–14178.

52 M. Rasouli, N. Yaghobi, S. Chitsazan and M. H. Sayyar, *Microporous Mesoporous Mater.*, 2012, **152**, 141–147.